Enhanced Ectasia Detection Using Corneal Tomography and Biomechanics

JOSÉ FERREIRA-MENDES, BERNARDO T. LOPES, FERNANDO FARIA-CORREIA, MARCELLA Q. SALOMÃO, SANDRA RODRIGUES-BARROS, AND RENATO AMBRÓSIO JR

• PURPOSE: To test the accuracy of the Tomographic and Biomechanical Index (TBI) for ectasia detection in an independent population from the original study.
• DESIGN: Retrospective case-control study.
• METHODS: SUBJECTS: Patients were grouped according to clinical diagnosis including corneal topography (front-surface curvature): Normal group, including 1 eye randomly selected from 312 patients with normal corneas; Keratoconus group, including 1 eye randomly selected from 118 patients with keratoconus; a nonoperated ectatic eye from 57 patients with very asymmetric ectasia (57 eyes, VAE-E group), and the nonoperated fellow eye with normal topography (57 eyes, VAE-NT group). MAIN OUTCOME MEASURES: The ability of TBI to distinguish normal and ectatic corneas; and comparison with other indexes, including the Belin/Ambrósio Deviation Index (BAD-DI) and the Corvis Biomechanical Index (CBI), considering the areas under receiver operating characteristic curves (AUCs).
• RESULTS: The AUC of the TBI was statistically higher than all other tested parameters (DeLong, $P < .001$). Considering all cases, the cut-off value of 0.335 for the TBI provided a sensitivity of 94.4% and a specificity of 94.9% (AUC = 0.988; 95% confidence interval [CI] 0.982–0.995). Considering the VAE-NT group, optimized TBI cut-off value of 0.295 provided a sensitivity of 89.5% and a specificity of 91.0% (AUC = 0.960; 95% CI 0.937–0.983).
• CONCLUSION: The TBI was more accurate than all parameters tested for differentiating normal from ectatic corneas. The TBI may epitomize ectasia susceptibility and distinguish cases with fruste disease from true unilateral cases among the eyes with normal-topography VAE. (Am J Ophthalmol 2019;197:7–16. © 2018 Elsevier Inc. All rights reserved.)

ACCURATE IDENTIFICATION OF MILD FORMS OF ectasia is fundamental prior to laser vision correction (LVC), because those cases are at very high risk for ectasia progression.[1,2] In addition, identifying mild forms of keratoconus is also important owing to the recent advances in managing the disease.[3] Placido disk–based corneal topography has been a classic method when screening for ectasia risk,[2] as it has been demonstrated to be sensitive for detecting keratoconus in candidates with unremarkable biomicroscopy and normal distance-corrected visual acuity (DCVA).[4,5] However, there are cases that develop ectasia notwithstanding a preoperative normal topography and no other identifiable risk factors.[6–9] Contrariwise, there are cases with preoperative irregular corneal topography that would have been excluded from LVC based on anterior surface characteristics, but that had proceeded with LASIK, with uneventful and stable outcomes.[10] Those clinical scenarios provide confirmation for the necessity for augmenting both sensitivity and specificity of ectasia risk assessment.[2,11]

Advances in corneal imaging technologies include corneal tomography and biomechanical assessments.[12] While the ideal cases for representing the eyes with high risk for ectasia progression are the preoperative state of the cases that developed ectasia after LVC procedures,[2,13,14] the fellow eyes with normal topography from patients with clinical ectasia in the ipsilateral eye have been commonly studied for providing higher accuracy than corneal topography maps themself.[15–23]

Ambrósio and associates described the Tomographic and Biomechanical Index (TBI), which combines Scheimpflug-based corneal tomography and biomechanics using artificial intelligence (AI) for optimizing ectasia detection.[24] The random forest method with leave-one-out cross-validation (RF/LOOCV) was the best model. In the original study, the TBI had 100% sensitivity and specificity for distinguishing normal (n = 480) and clinical ectasia eyes (n = 276), with 0.79 as cut-off. The optimized cut-off value of 0.29 provided 90.4% sensitivity for the very asymmetric ectasia with normal topography (VAE-NT)

AJO.com Supplemental Material available at AJO.com.

Accepted for publication Aug 31, 2018.

From the Rio de Janeiro Corneal Tomography and Biomechanics Study Group, Rio de Janeiro, Brazil (J.F.-M., B.L., F.F.-C., M.Q.S., R.A.); Ophthalmology Department, Hospital de Braga, Braga, Portugal (J.F.-M., F.F.-C.); Life and Health Sciences Research Institute (ICVS), School of Health Sciences, University of Minho, Braga, Portugal (J.F.-M., F.F.-C.); ICVS/3B's - PT Government Associate Laboratory, Braga/Guimarães, Portugal (J.F.-M., F.F.-C.); Instituto de Olhos Renato Ambrósio, Rio de Janeiro, Brazil (B.L., M.Q.S., R.A.); Department of Ophthalmology and Visual Sciences, Federal University of São Paulo, São Paulo, Brazil (B.L., M.Q.S., R.A.); Barra Vision Center, Rio de Janeiro, Brazil (M.Q.S.); Hospital Garcia de Orta, Almada, Portugal (S.R.-B.); and Department of Ophthalmology, Federal University of the State of Rio de Janeiro, Rio de Janeiro, Brazil (R.A.).

Inquiries to Renato Ambrósio Jr, Instituto de Olhos Renato Ambrósio, Rua Conde de Bonfim 211/712, Rio de Janerio, RJ, 20.520-050, Brazil; e-mail: dr.renatoambrosio@gmail.com

0002-9394/$36.00
https://doi.org/10.1016/j.ajo.2018.08.054

TABLE 1. Demographic Characteristics of Study Group

Group	N					Average Subject Age (y) ± Standard Deviation (Range)
	Total	OD	OS	Male	Female	
Normal	312	156	156	127	185	39.33 ± 17.18 (7.73–85.52)
Keratoconus	118	50	68	64	54	36.71 ± 17.20 (14.58–82.14)
Very asymmetric ectasia – ectatic	57	22	35	34	23	33.26 ± 14.41 (14.16–73.09)
Very asymmetric ectasia – normal topography		35	22			

cases (n = 94), with 96% specificity.[24] Nevertheless, while the TBI had exceeding accuracy over all other parameters tested, there is a fundamental need for external validations.[25] The goal of this study is to provide an external validation for the TBI, in an independent population from the one used for creating or training the parameter in the original study.

METHODS

PATIENTS FROM INSTITUTO DE OLHOS RENATO AMBRÓSIO, Rio de Janeiro, Brazil, were enrolled in this retrospective case-control study. All case-control studies are observational. The ethics committee of the Federal University of São Paulo approved this retrospective research study, which was conducted in accordance with the tenets of the 1964 Declaration of Helsinki (revised in 2000).

The eyes were divided into 4 groups, according to the clinical presentation. The Normal group included 1 eye randomly selected from patients with normal corneas. The Keratoconus group included 1 eye randomly selected from patients with keratoconus. In these 2 groups, 1 eye was randomly included per patient to avoid selection bias related to the use of both eyes from the same patient.[25] Both eyes from patients with very asymmetric ectasia (VAE) entered the study. However, eyes that had 1 or more surgical procedures (ie, cross-linking or intrastromal ring segment implantation) were not included this study because those procedures alter the biomechanical properties of the cornea. Thereby the VAE-E group was comprised from ectatic eyes that had no previous surgery and the VAE-NT group included the fellow eyes of these patients that had normal topography.

All patients had a comprehensive ophthalmic examination, including the Corvis ST (Oculus Optikgeräte GmbH, Wetzlar, Germany) and Pentacam HR (Oculus Optikgeräte GmbH, Wetzlar, Germany) examinations with acceptable quality for proper analysis. Soft contact lens wear was discontinued for at least 3 days prior to the examination and rigid or hybrid contact lenses were discontinued for a minimum period of 3 weeks. The inclusion criteria for being a normal case were to have normal corneas on the general eye examination in both eyes, including normal slit-lamp biomicroscopy, corrected distance visual acuity of 20/20 or better, overall subjective normal topography and tomography examinations with no previous surgery, and no use of topical medications other than artificial tears. The criterion for being a keratoconus case was the diagnosis of clinical ectasia in both eyes, without any previous ocular procedures (ie, LVC, intrastromal segment rings, cross-linking). The criteria for clinical diagnosis of ectasia included topographic characteristics (ie, skewed asymmetric bow-tie or inferior steepening) and at least 1 slit-lamp finding (ie, Munson sign, Vogt striae, Fleischer ring, apical thinning, or Rizzuti sign).[26] Patients were considered to be very asymmetric if the diagnosis of ectasia was confirmed in 1 eye based on the previously described criteria and the fellow eye had a normal front surface curvature (topometric) map. Objective criteria for considering normal topography were rigorously applied for defining the cases of VAE-NT, including objective front surface curvature metrics derived from Pentacam HR, such as a keratoconus percentage index (KISA%) score lower than 60 and a paracentral inferior-superior (I-S value) asymmetry value at 6 mm (3 mm radii) less than 1.45.[27] These criteria avoid problems related to the subjectivity and interexaminer and intraexaminer variability of the classification of topographic maps.

Experienced technicians took all measurements from the Corvis ST and Pentacam HR. Proper examination quality was ensured by a manual, frame-by-frame analysis of each examination by an independent masked examiner to ensure quality of each acquisition, including good edge detection over the whole deformation response or rotating Scheimpflug images, with the exclusion of severe alignment errors (x-direction) and blinking errors.[28] Raw data from the Pentacam HR and Corvis ST were exported to a custom spreadsheet using research software, which is currently available on the instrument. Statistical analyses were performed by different software packages: MedCalc Statistical Software (version 16.8.4; MedCalc, Ostend, Belgium) and SPSS (version 23; IBM Corporation, Armonk, New York, USA). Analysis of variance (ANOVA) was used to test differences for age among the groups. Considering all indices in the keratoconus group were non-normally distributed, the analyzed parameters were compared among the groups using the nonparametric Kruskal-Wallis test,

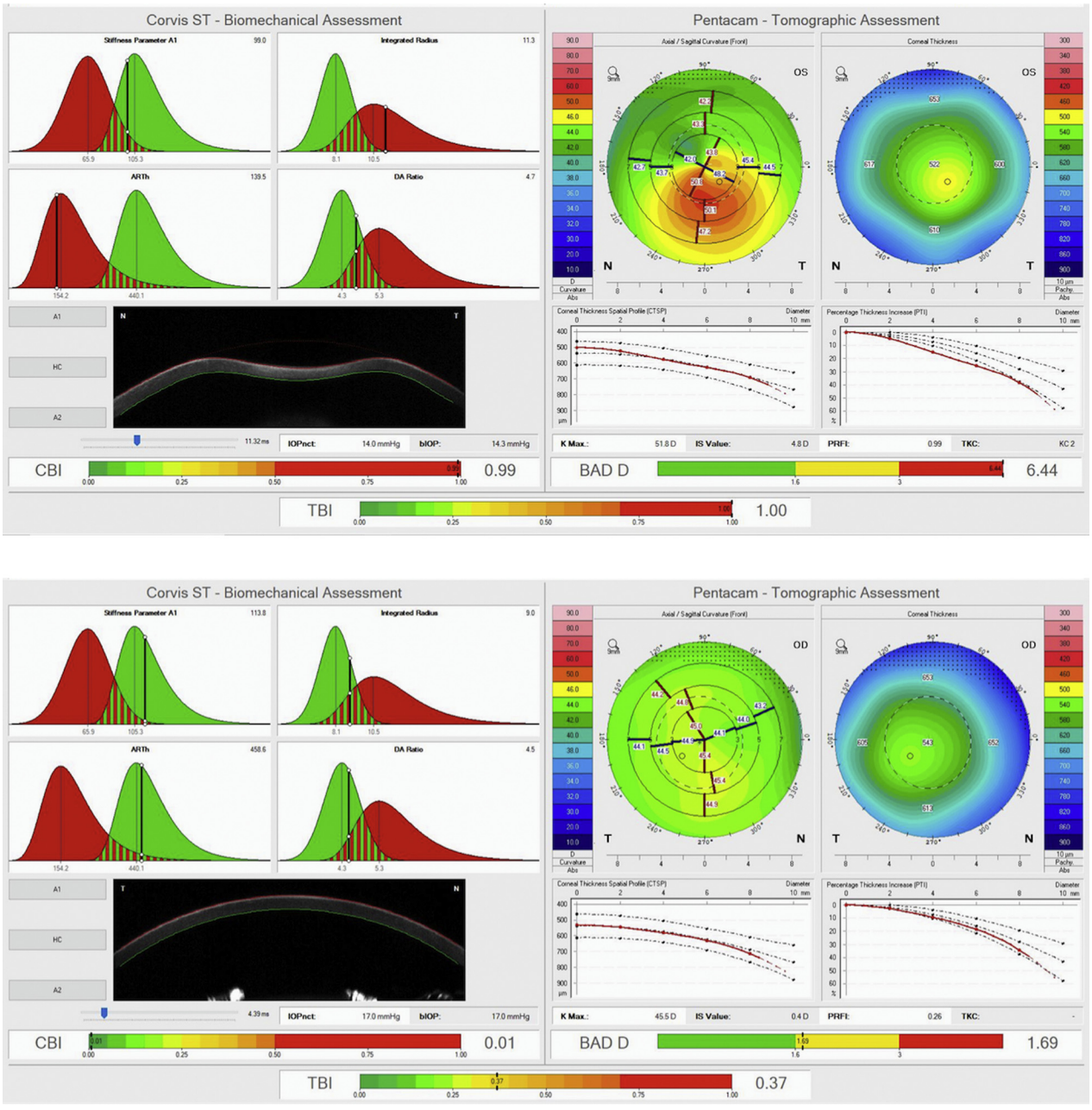

FIGURE 1. Patient with very asymmetric ectasia with clinical ectasia (VAE-E) in the right eye and very asymmetric ectasia with normal topography (VAE-NT) in the left eye. (Top) Tomography and biomechanical assessment of the eye (OD) with mild ectatic presentation (VAE-E). (Bottom) Tomography and biomechanical assessment of the fellow eye (OS) of the same patient, with VAE-NT.

followed by the post hoc Dunn test to compare each pair of groups. The discriminative ability of each parameter was assessed by receiver operating characteristic (ROC) curves. For each parameter tested, the area under the ROC curve (AUROC) was calculated and the best cut-off value that yielded the highest accuracy was determined along with sensitivity and specificity. Pairwise comparisons of the AUROC were accomplished with the nonparametric approach as described by DeLong and associates for comparing the performance of diagnostic tests.[29]

RESULTS

A TOTAL OF 544 EYES (1 EYE RANDOMLY SELECTED FROM 312 normal patients [Normal group] and from 118 patients with keratoconus [Keratoconus group]; 57 eyes with very asymmetric ectasia [VAE-E group]; and 57 fellow eyes with normal topography [VAE-NT group]) of 487 patients were included. Demographic characteristics are presented in Table 1. Ages ranged from 7 to 85 years, similarly to the original study. In the normal group, central and minimal corneal

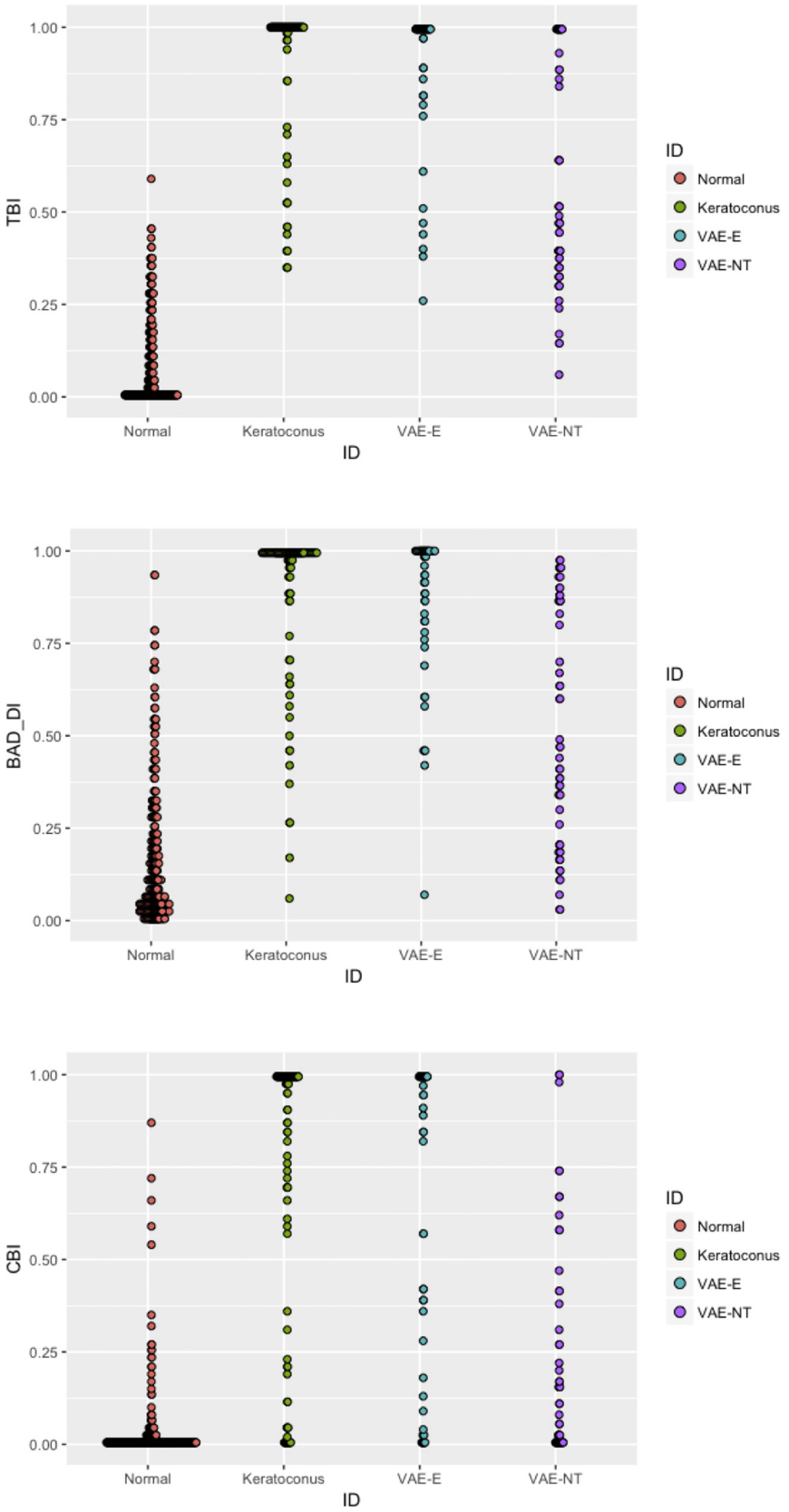

FIGURE 2. Dot plots showing the distribution of metric values across the normal (n = 312), keratoconus (KC) (n = 118), very asymmetric ectasia with clinical ectasia (VAE-E), and very asymmetric ectasia with normal topography (VAE-NT) (n = 57) groups. BAD-DI = Belin/Ambrósio Deviation normalized index; CBI = Corvis biomechanical index; TBI = tomographic and biomechanical index.

TABLE 2. Descriptive Analysis of Topometric, Tomographic and Biomechanical Parameters

	Normal Group (N = 312)	Keratoconus Group (N = 118)	Very Asymmetric Ectasia – Ectatic Group (N = 57)	Very Asymmetric Ectasia – Normal Topography Group (N = 57)
Paracentral inferior-superior asymmetry value, Diopters	0.08 ± 0.54 (-1.44 to 1.71)	4.21 ± 3.28 (-1.42 to 14.50)	2.64 ± 3.31 (-7.08 to 11.57)	0.60 ± 0.58 (-0.93 to 1.41)
Maximum axial curvature of the front surface, Diopters	44.50 ± 1.54 (39.65 to 49.71)	51.33 ± 4.88 (43.28 to 79.35)	49.98 ± 7.13 (42.86 to 77.97)	44.89 ± 1.25 (42.18 to 47.08)
Keratoconus percentage index, microns	11.56 ± 17.01 (0.33 to 164.43)	661.34 ± 3402.43 (0.68 to 36 671.89)	865.88 ± 2821.76 (0.37 to 15 008.54)	14.81 ± 16.46 (0.33 to 54.37)
Minimal pachymetric value, microns	544.99 ± 30.15 (472.00 to 636.00)	480.27 ± 44.88 (336.00 to 590.00)	491.54 ± 50.69 (328.00 to 617.00)	515.75 ± 30.88 (447.00 to 612.00)
Simulated pachymetric value central corneal	522.33 ± 20.09 (444.83 to 583.00)	483.91 ± 44.58 (156.65 to 543.45)	488.18 ± 38.69 (379.42 to 581.05)	508.72 ± 20.92 (456.33 to 565.47)
Deformation amplitude ratio apex and 2 mm	4.39 ± 0.39 (3.22 to 5.37)	5.25 ± 0.75 (3.84 to 7.81)	5.18 ± 0.90 (3.54 to 8.21)	4.74 ± 0.44 (3.63 to 5.73)
Inverse max inverse radius high concavity, mm^{-1}	8.59 ± 0.99 (5.57 to 11.99)	10.71 ± 2.03 (6.01 to 18.23)	10.64 ± 2.18 (5.27 to 18.80)	9.46 ± 0.91 (6.60 to 11.27)
K1, Diopters	42.76 ± 1.44 (38.50 to 47.30)	44.47 ± 3.44 (33.30 to 65.30)	44.05 ± 3.78 (39.40 to 59.40)	42.87 ± 1.43 (39.20 to 45.80)
K2, Diopters	43.94 ± 1.48 (39.40 to 48.00)	47.57 ± 3.58 (40.70 to 69.30)	46.57 ± 5.12 (42.20 to 67.10)	43.99 ± 1.44 (40.50 to 46.60)
Elevation front best fit sphere 8 mm apex, microns	1.38 ± 1.00 (-1.00 to 4.00)	5.92 ± 7.86 (-11.00 to 64.00)	5.73 ± 8.74 (-2.00 to 53.00)	1.60 ± 1.53 (-3.00 to 6.00)
Elevation back best fit sphere 8 mm apex, microns	1.64 ± 2.66 (-4.00 to 11.00)	13.45 ± 17.46 (-23.00 to 121.00)	11.30 ± 16.78 (-10.00 to 82.00)	2.04 ± 3.50 (-4.00 to 10.00)
Elevation front best fit sphere 8 mm thinnest, microns	1.78 ± 1.68 (-6.00 to 9.00)	14.84 ± 13.70 (-5.00 to 89.00)	11.14 ± 12.04 (-3.00 to 54.00)	2.68 ± 1.88 (-3.00 to 8.00)
Elevation back best fit sphere 8 mm thinnest, microns	1.64 ± 2.66 (-4.00 to 11.00)	36.66 ± 28.99 (-1.00 to 203.00)	33.96 ± 32.71 (4.00 to 204.00)	9.82 ± 5.73 (-2.00 to 25.00)
Elevation front best fit sphere 8 mm maximum 4 mm zone, microns	1.78 ± 1.68 (-6.00 to 9.00)	20.31 ± 14.06 (3.00 to 79.00)	15.61 ± 13.23 (2.00 to 59.00)	5.23 ± 3.17 (2.00 to 22.00)
Elevation back best fit sphere 8 mm maximum 4 mm zone, microns	12.73 ± 5.20 (0.00 to 38.00)	43.48 ± 26.07 (7.00 to 147.00)	37.59 ± 23.10 (11.00 to 101.00)	15.18 ± 5.67 (7.00 to 31.00)
Tomographic and Biomechanical Index	0.09 ± 0.12 (0.00 to 0.59)	0.92 ± 0.18 (0.34 to 1.00)	0.91 ± 0.19 (0.26 to 1.00)	0.60 ± 0.31 (0.06 to 1.00)
Belin/Ambrósio Deviation Index	0.87 ± 0.60 (-0.77 to 2.81)	5.87 ± 4.21 (0.67 to 30.73)	5.27 ± 4.64 (0.73 to 26.15)	1.81 ± 0.71 (0.39 to 3.29)
Corvis Biomechanical Index	0.03 ± 0.10 (0.00 to 0.87)	0.71 ± 0.40 (0.00 to 1.00)	0.60 ± 0.43 (0.00 to 1.00)	0.21 ± 0.29 (0.00 to 1.00)

K1 = flattest central keratometry; K2 = steepest central keratometry.

TABLE 3. Results of Receiver Operating Characteristic Curve Analysis

Parameter	Area Under Curve	95% Confidence Interval	Sensitivity	Specificity	Cut-off
Normal vs Keratoconus, Very asymmetric ectasia – ectatic, and Very asymmetric ectasia – normal topography groups					
Tomographic and Biomechanical Index	0.988	0.982–0.995	94.4%	94.9%	0.335
Belin/Ambrósio Deviation Index	0.946	0.927–0.964	89.2%	86.2%	0.345
Corvis Biomechanical Index	0.864	0.832–0.896	70.7%	93.3%	0.085
Normal vs Keratoconus and Very asymmetric ectasia – normal topography groups					
Tomographic and Biomechanical Index	0.998	0.995–1.000	97.1%	98.1%	0.385
Belin/Ambrósio Deviation Index	0.981	0.967–0.992	91.4%	95.5%	0.575
Corvis Biomechanical Index	0.893	0.859–0.927	78.3%	93.3%	0.085
Normal vs Very asymmetric ectasia – normal topography group					
Tomographic and Biomechanical Index	0.960	0.937–0.983	89.5%	91.0%	0.295
Belin/Ambrósio Deviation Index	0.839	0.783–0.894	68.4%	84.6%	0.325
Corvis Biomechanical Index	0.775	0.705–0.849	77.2%	67.9%	0.005

thickness values and maximum (Kmax) keratometric values were normally distributed among normal eyes (Kolmogorov-Smirnov; $P > .50$).

All frank ectasia cases (Keratoconus and VAE-E groups) had abnormalities detected by corneal topography that fulfilled criteria for diagnosis.[26,27] All eyes in the VAE-NT group were objectively determined to have normal topography: I-S value lower than 1.45 diopters; KISA% score lower than 60; no positive topometric classification for keratoconus value.[27] Figure 1 presents a case of a patient with VAE-E (Top) in the right eye and VAE-NT (Bottom) in the left eye.

Considering that TBI and Corvis Biomechanical Index (CBI) were programmed to have their output values as a continuous number ranging from zero to 1,[24,30] a linear regression analysis function was created only using the Belin/Ambrósio Deviation (BAD-D) as the input parameter to calculate the Belin/Ambrósio Deviation Index (BAD-DI) in order to facilitate comparisons. Figure 2 displays the dot-plot graphs for the TBI, BAD-DI, and CBI. Table 2 includes the mean ± standard deviation, median, and range (minimum to maximum) for the main parameters, including the BAD-D, CBI, and TBI. Results of Kruskal–Wallis 1-way ANOVA demonstrated differences among the studied groups for all studied parameters ($P < .000001$), which was confirmed by Jonckheere-Terpstra trend test ($P < .00001$). Post hoc Dunn test results were similar for all parameters, confirming differences among all paired groups ($P < .001$), with the exception of the comparison between keratoconic and ectatic eyes from the very asymmetric cases (Keratoconus group vs VAE-E group). Table 3 summarizes the results of the ROC curves. The analysis was performed to test the discriminating abilities to separate Normal cases vs all diseased cases (Keratoconus + VAE-E + VAE-NT) (Figure 3, Top); Normal cases vs cases with frank ectasia (K + VAE-E) (Figure 3, Middle); and normal cases vs cases with the supposed subclinical cases (VAE-NT) (Figure 3, Bottom).

The AUC of the TBI for detecting ectasia and ectasia susceptibility (Keratoconus, VAE-E, and VAE-NT groups) was 0.988. The cut-off value of 0.335 presented a sensitivity of 94.4% and a specificity of 94.9% (Table 3). This combined parameter presented a statistically higher AUC compared to the other parameters (DeLong et al., $P < .05$).[29] The TBI presented an AUC of 0.998 (a sensitivity of 97.1% and a specificity of 98.1%) to detect frank ectasia cases (keratoconus and VAE-E groups), considering an optimized cut-off value of 0.385. Considering the ability to detect the eyes with normal topography from patients with clinical ectasia in the fellow eye (VAE-NT group), an optimization of cut-off value to 0.295 provided an AUROC of 0.960, with a sensitivity of 89.5% and a specificity of 91.0%.

DISCUSSION

THE REPORTED INCIDENCE OF UNILATERAL KERATOCONUS (or better, ectasia) in the literature varies depending on the methods used for diagnosis.[31] In 1946 Amsler reported an incidence of 22% using a photographic placido disc,[32] in 1982 Krachmer and associates reported an incidence of 14.3% using photokeratoscopy in addition to other clinical findings,[33] in 1986 Kennedy and associates reported an incidence of 41% using retroillumination techniques and keratometry,[34] and in 1993 Rabinowitz and associates reported an incidence of 4% using videokeratography and I-S values.[31] In fact, the 2015 consensus stated that true unilateral keratoconus does not exist, and that ectasia may occur because of mechanical causes.[35] It is fundamental to consider that normal topography does not

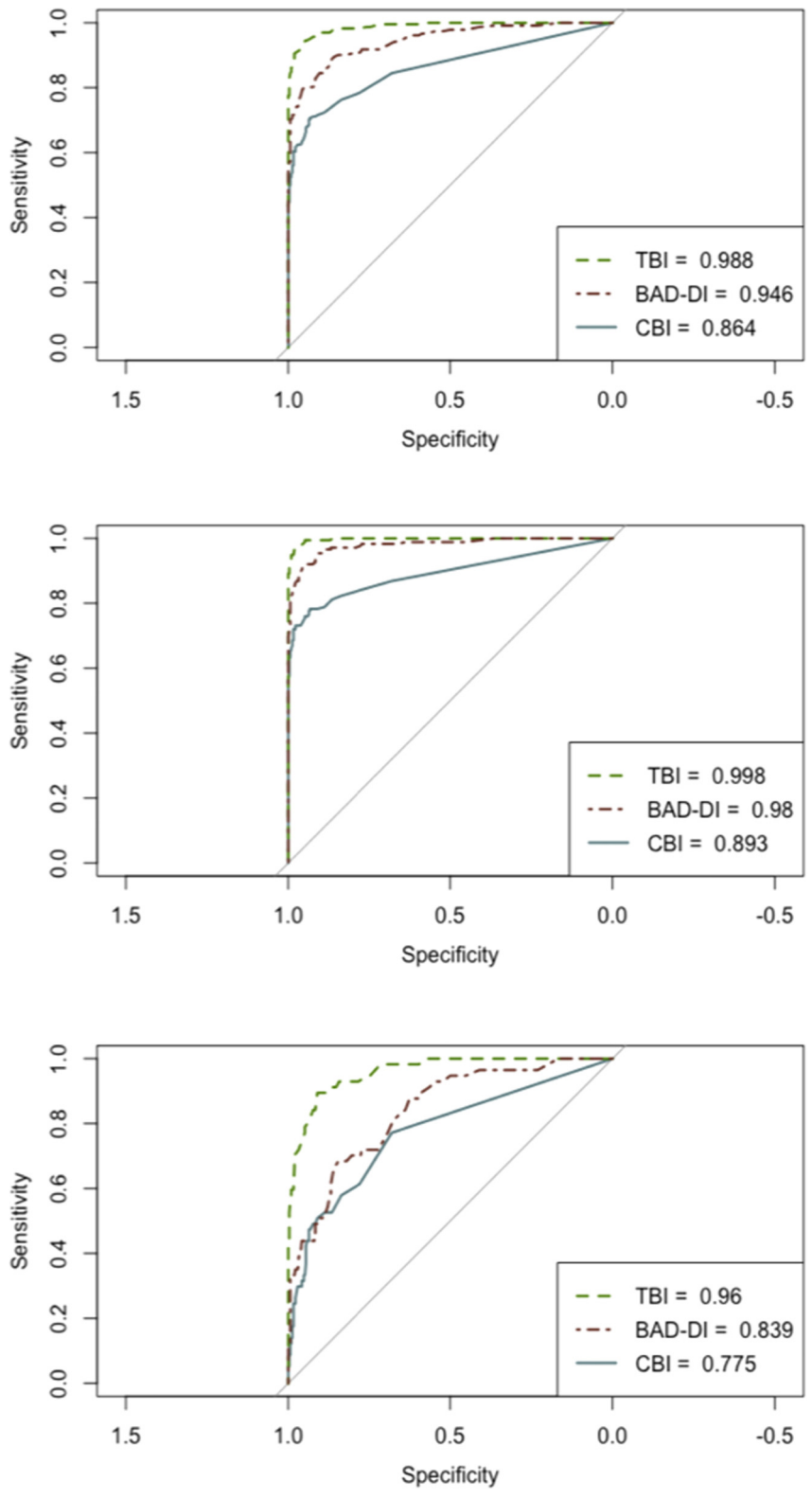

FIGURE 3. Receiver operating characteristic (ROC) and separation curves for the different groups: (Top) Normal (N) vs Keratoconus (K), very asymmetric ectasia with clinical ectasia (VAE-E), and very asymmetric ectasia with normal topography (VAE-NT) groups; (Middle) N vs K and VAE-E groups; and (Bottom) N vs VAE-NT group. BAD-DI = Belin/Ambrósio Deviation normalized index; CBI = Corvis Biomechanical Index; TBI = Tomographic and Biomechanical Index. Note that BAD-D and BAD-DI had identical ROC and separation curves, as BAD-DI is a normalized function of BAD-D with values from zero to 1.[24]

exclude mild or early ectatic corneal disease, longitudinal data having shown that over 20% of the fellow eyes in unilateral keratoconus patients progressed to clinical keratoconus.[2,36] The progressive thinning and ectasia can be exacerbated by factors such as eye rubbing and corneal refractive surgery[37]; also, a genetic heritage seems to express itself in a variable fashion.[36,37]

In a previous study,[24] the TBI was developed using the RF artificial intelligence method and its validity was confirmed by the LOOCV technique. In the present study, we provide external validation for the accuracy of the TBI for detecting very mild forms of ectasia, such as subclinical forms in patients with apparently normal topography, by applying it to a naïve group of patients, independent from the original one. This study included a large cohort of patients with normal corneas and different levels of ectatic corneal disease. To avoid selection bias related to the use of both eyes from the same patient, we included 1 randomly selected eye per patient in the normal and keratoconus groups. Fifty-seven patients had 1 eye assigned to the VAE-E group and the other eye to the VAE-NT group; these cases were by definition very asymmetric, which avoids issues related to enantiomorphism or similarities between right and left eyes. Considering the limitations of subjective interpretation of corneal topography maps, we were restricted to applying front surface curvature indices, as described by Rabinowitz and Rasheed, for objectively defining the inclusion criteria of the VAE- NT group.[27]

There is controversy regarding the existence of unilateral ectasia. The current consensus states that true unilateral keratoconus does not exist; however, it must be considered that true unilateral ectasia cases may exist, namely secondary to mechanical stress induced by eye rubbing. In fact, these ideas are in conformity with the 2-hit hypothesis that arises with the concept that ectasia results from an underlying genetic predisposition along with external environmental factors, including eye rubbing and atopy.

The major goal of the present study is to perform an external validation of the TBI for assessing inherent susceptibility of the cornea to ectasia. Despite being performed at the same center, this study enrolled an independent and distinct group of patients, when compared to the original report of TBI. Our current study includes a significant number of mild ectatic cases, in order to stress the ability of TBI to identify susceptibility to ectasia in the fellow normal topography eye (VAE-NT). Similar to the original study, the TBI demonstrated a higher accuracy for detecting ectatic corneal diseases than all other enrolled tomographic and biomechanical parameters (Figures 2 and 3, Table 3). The AUROC of the TBI was significantly higher than CBI for the following separations: Normal vs Keratoconus, VAE-E, and VAE-NT ($P < .001$); Normal vs Keratoconus and VAE-E ($P < .0001$); and Normal vs VAE-NT ($P < .001$); and was significantly higher than the BAD-DI for Normal vs Keratoconus, VAE-NT, and VAE-E ($P < .001$) and Normal vs VAE-NT ($P < .001$). For comparison between Normal vs Keratoconus, VAE-E, and VAE-NT, the original report metrics were higher than those at this time: TBI 0.996 vs 0.988; BAD-DI 0.956 vs 0.946; CBI 0.937 vs 0.864. The diminution is explained with the higher number of mild ectatic cases accepted as VAE-E on the presenting study. Interestingly, despite the diminution, TBI still performed better than BAD-D and CBI on ectasia screening. Similar data are also present on comparison between Normal vs Keratoconus and VAE-E (TBI 1.000 vs 0.998; BAD-DI 0.997 vs 0.981; CBI 0.977 vs 0.893) and between Normal vs VAE-NT (TBI 0.985 vs 0.960; BAD-DI 0.838 vs 0.839; CBI 0.822 vs 0.775).

Differentiating a normal population from ectatic eyes is fundamental on refractive surgery screening process, as the risk of developing ectasia after LVC increases according to its biomechanical impact.[38] Patients with increased susceptibility for ectasia may not reveal risk factors based on standard screening protocols and are represented by the VAE-NT group. Regarding the purpose of this study, the TBI was demonstrated to be the most accurate parameter. For a cutoff of 0.295, and with an AUC of 0.960, TBI had a sensitivity of 89.5% and a specificity of 91.0% to differentiate normal corneas from normal topography eyes of a patient with the fellow eye with very asymmetric ectasia. It is possible that some of these cases indeed represent normal eyes from patients with unilateral ectasia.[35] This may be particularly true for cases of unilateral ectasia induced owing to environmental confounding factors. Although this is expected to be relatively rare, it is also possible that some eyes with a normal clinical examination (including corneal topography and tomography) have mild or susceptible forms of ectasia that may progress only after LVC procedures. A longitudinal follow-up of these patients would allow understanding of the stability of the biomechanical properties and the shape of their corneas, increasing the preciseness of the inclusion in the normal group.

An ideal study would prospectively include preoperative biomechanical and tomographic data of those corneas that progressed to clinical ectasia after LVC. Although this is not possible, the study involving very asymmetric ectasia cases is the most suitable for developing and demonstrating enhanced ability for ectasia diagnosis. Other studies to externally validate the TBI are ongoing, as this is a current objective of active research.

FUNDING/SUPPORT: NO FUNDING OR GRANT SUPPORT. FINANCIAL DISCLOSURES: RENATO AMBRÓSIO JR IS A CONSULTANT for Oculus GmbH (Wetzlar, Germany), as well as Alcon, Allergan, and ZEISS. The following authors have no financial disclosures: José Ferreira-Mendes, Bernardo Lopes, Fernando Faria-Correia, Marcella Q. Salomão, and Sandra Rodrigues-Barros. All authors attest that they meet the current ICMJE criteria for authorship.

REFERENCES

1. Binder PS, Lindstrom RL, Stulting RD, et al. Keratoconus and corneal ectasia after LASIK. *J Refract Surg* 2005;21(6):749–752.
2. Ambrosio R Jr, Randleman JB. Screening for ectasia risk: what are we screening for and how should we screen for it? *J Refract Surg* 2013;29(4):230–232.
3. Seiler T. The paradigm change in keratoconus therapy. *Indian J Ophthalmol* 2013;61(8):381.
4. Ambrosio R Jr, Klyce SD, Wilson SE. Corneal topographic and pachymetric screening of keratorefractive patients. *J Refract Surg* 2003;19(1):24–29.
5. Torricelli AA, Bechara SJ, Wilson SE. Screening of refractive surgery candidates for LASIK and PRK. *Cornea* 2014;33(10):1051–1055.
6. Klein SR, Epstein RJ, Randleman JB, Stulting RD. Corneal ectasia after laser in situ keratomileusis in patients without apparent preoperative risk factors. *Cornea* 2006;25(4):388–403.
7. Randleman JB, Trattler WB, Stulting RD. Validation of the Ectasia Risk Score System for preoperative laser in situ keratomileusis screening. *Am J Ophthalmol* 2008;145(5):813–818.
8. Randleman JB, Woodward M, Lynn MJ, Stulting RD. Risk assessment for ectasia after corneal refractive surgery. *Ophthalmology* 2008;115(1):37–50.
9. Ambrosio R Jr, Dawson DG, Salomao M, Guerra FP, Caiado AL, Belin MW. Corneal ectasia after LASIK despite low preoperative risk: tomographic and biomechanical findings in the unoperated, stable, fellow eye. *J Refract Surg* 2010;26(11):906–911.
10. Reinstein DZ, Archer TJ, Gobbe M. Stability of LASIK in topographically suspect keratoconus confirmed non-keratoconic by Artemis VHF digital ultrasound epithelial thickness mapping: 1-year follow-up. *J Refract Surg* 2009;25(7):569–577.
11. Ambrósio R Jr, MW B. Enhanced screening for ectasia risk prior to laser vision correction. *Int J Keratoconus Ectatic Corneal Dis* 2017;6(1):23–33.
12. Ambrosio R Jr, Nogueira LP, Caldas DL, et al. Evaluation of corneal shape and biomechanics before LASIK. *Int Ophthalmol Clin* 2011;51(2):11–38.
13. Ambrosio R Jr, Dawson DG, Belin MW. Association between the percent tissue altered and post-laser in situ keratomileusis ectasia in eyes with normal preoperative topography. *Am J Ophthalmol* 2014;158(6):1358–1359.
14. Ambrósio R Jr, Ramos I, Lopes B, et al. Assessing ectasia susceptibility prior to LASIK: the role of age and residual stromal bed (RSB) in conjunction to Belin-Ambrósio deviation index (BAD-D). *Rev Bras Oftalmol* 2014;73:75–80.
15. Saad A, Gatinel D. Topographic and tomographic properties of forme fruste keratoconus corneas. *Invest Ophthalmol Vis Sci* 2010;51(11):5546–5555.
16. Arbelaez MC, Versaci F, Vestri G, Barboni P, Savini G. Use of a support vector machine for keratoconus and subclinical keratoconus detection by topographic and tomographic data. *Ophthalmology* 2012;119(11):2231–2238.
17. Smadja D, Touboul D, Cohen A, et al. Detection of subclinical keratoconus using an automated decision tree classification. *Am J Ophthalmol* 2013;156(2):237–246 e231.
18. Muftuoglu O, Ayar O, Ozulken K, Ozyol E, Akinci A. Posterior corneal elevation and back difference corneal elevation in diagnosing forme fruste keratoconus in the fellow eyes of unilateral keratoconus patients. *J Cataract Refract Surg* 2013;39(9):1348–1357.
19. Ambrosio R Jr, Valbon BF, Faria-Correia F, Ramos I, Luz A. Scheimpflug imaging for laser refractive surgery. *Curr Opin Ophthalmol* 2013;24(4):310–320.
20. Luz A, Lopes B, Hallahan KM, et al. Enhanced combined tomography and biomechanics data for distinguishing forme fruste keratoconus. *J Refract Surg* 2016;32(7):479–494.
21. Shetty R, Rao H, Khamar P, et al. Keratoconus screening indices and their diagnostic ability to distinguish normal from ectatic corneas. *Am J Ophthalmol* 2017;181:140–148.
22. Vinciguerra R, Ambrosio R Jr, Roberts CJ, Azzolini C, Vinciguerra P. Biomechanical characterization of subclinical keratoconus without topographic or tomographic abnormalities. *J Refract Surg* 2017;33(6):399–407.
23. Reinstein DZ, Archer TJ, Urs R, Gobbe M, RoyChoudhury A, Silverman RH. Detection of keratoconus in clinically and algorithmically topographically normal fellow eyes using epithelial thickness analysis. *J Refract Surg* 2015;31(11):736–744.
24. Ambrosio R Jr, Lopes BT, Faria-Correia F, et al. Integration of Scheimpflug-based corneal tomography and biomechanical assessments for enhancing ectasia detection. *J Refract Surg* 2017;33(7):434–443.
25. Lopes B, Ramos ICdO, Ribeiro G, et al. Bioestatísticas: conceitos fundamentais e aplicações práticas. *Rev Bras Oftalmol* 2014;73:16–22.
26. Rabinowitz YS. Keratoconus. *Surv Ophthalmol* 1998;42(4):297–319.
27. Rabinowitz YS, Rasheed K. KISA% index: a quantitative videokeratography algorithm embodying minimal topographic criteria for diagnosing keratoconus. *J Cataract Refract Surg* 1999;25(10):1327–1335.
28. Ramos IC, Correa R, Guerra FP, et al. Variability of subjective classifications of corneal topography maps from LASIK candidates. *J Refract Surg* 2013;29(11):770–775.
29. DeLong ER, DeLong DM, Clarke-Pearson DL. Comparing the areas under two or more correlated receiver operating characteristic curves: a nonparametric approach. *Biometrics* 1988;44(3):837–845.
30. Vinciguerra R, Ambrosio R Jr, Elsheikh A, et al. Detection of keratoconus with a new biomechanical index. *J Refract Surg* 2016;32(12):803–810.

31. Rabinowitz YS, Nesburn AB, McDonnell PJ. Videokeratography of the fellow eye in unilateral keratoconus. *Ophthalmology* 1993;100(2):181–186.
32. Amsler M. Kératocône classique et kératocône fruste; arguments unitaires. *Ophthalmologica* 1946;111(2-3):96–101.
33. Krachmer JH, Feder RS, Belin MW. Keratoconus and related noninflammatory corneal thinning disorders. *Surv Ophthalmol* 1984;28(4):293–322.
34. Kennedy RH, Bourne WM, Dyer JA. A 48-year clinical and epidemiologic study of keratoconus. *Am J Ophthalmol* 1986;101(3):267–273.
35. Gomes JA, Rapuano CJ, Belin MW, Ambrosio R Jr. Group of Panelists for the Global Delphi Panel of Keratoconus and Ectatic Diseases. Global consensus on keratoconus diagnosis. *Cornea* 2015;34(12):e38–39.
36. Li X, Yang H, Rabinowitz YS. Keratoconus: classification scheme based on videokeratography and clinical signs. *J Cataract Refract Surg* 2009;35(9):1597–1603.
37. Klyce SD. Chasing the suspect: keratoconus. *Br J Ophthalmol* 2009;93(7):845–847.
38. Roberts CJ, Dupps WJ Jr. Biomechanics of corneal ectasia and biomechanical treatments. *J Cataract Refract Surg* 2014;40(6):991–998.